ISSN- 0102-9010

DICHOTOMIC SPERMIOGENESIS IN *Euptoieta hegesia* (LEPIDOPTERA: NYMPHALIDAE)

Karina Mancini and Heidi Dolder

Department of Cell Biology, Institute of Biology, State University of Campinas (UNICAMP), Campinas, SP, Brazil.

ABSTRACT

Butterflies and moths produce enucleate (apyrene) and nucleate (eupyrene) spermatozoa. However, most studies of lepidopteran spermatogenesis and spermiogenesis have used only larvae and pupae. In this work, we used light and transmission electron microscopy to examine spermiogenesis in males of the butterfly *Euptoieta hegesia*. Only adult males were used, because this species has a long adult lifespan during which all cell stages can be observed. Male *E. hegesia* had a single fused testis with cysts that exclusively contained either apyrene or eupyrene cells. The main events of apyrene spermiogenesis included the formation, transformation and elimination of micronuclei, dense cap formation, the development of mitochondrial derivatives and tail elongation. Eupyrene spermiogenesis involved acrosome formation, nuclear condensation and elongation, extracellular appendage development, formation of mitochondrial derivatives and tail elongation. The pattern and events of apyrene and eupyrene spermiogenesis in *E. hegesia* corroborate and complement data in the literature, particularly with regard to the intermediate developmental stages of some structures, such as the acrosome, axoneme and extracellular appendages.

Key words: Apyrene, eupyrene, spermiogenesis, structure, ultrastructure

INTRODUCTION

Sperm polymorphism exists in several invertebrate groups, such as rotifers, turbellarians, mollusks and insects [5]. In insects, this polymorphism occurs in many orders and the spermatozoa can differ in length (Diptera), chromosome number (Coleoptera) or morphology (Lepidoptera, Hemiptera, Heteroptera and Hymenoptera) [14,15]. A well-known case of sperm polymorphism in Lepidoptera involves the production of apyrene (enucleate) and eupyrene (nucleate) spermatozoa, which are morphologically and functionally different. This phenomenon has been reported for all butterfly and moth species studied so far, except for the basal group Micropterygidae, in which only eupyrene spermatozoa occur [12,35]. The two types of spermatozoa differ by the absence or presence of a nucleus and also in their length, mitochondrial derivative structures, and the absence or presence of an acrosome, glycocalyx and extracellular appendages.

Apyrene and eupyrene sperm are also functionally distinct. Eupyrene spermatozoa fertilize the egg while apyrene spermatozoa may be only indirectly involved in this process since they are devoid of a nucleus. Some studies have suggested that the function of apyrene spermatozoa is to dissociate the eupyrene cyst [29] or to transport eupyrene sperm bundles to the female tract [8,9,30]. However, more recent investigations have indicated that apyrene cells are involved in sperm competition [1,33,34,36,37], as originally proposed by Silberglied [32] and Drummond [4].

Although the two sperm types are produced in different developmental phases, with eupyrene spermiogenesis beginning first, both occur simultaneously in adults [6,16,22]. This study describes spermiogenesis in adult males of *E. hegesia*. Only males were used because this species has a long adult lifespan of about 14 days, during which all cell stages can be observed.

MATERIAL AND METHODS

Approximately 50 adults of the butterfly *Euptoieta hegesia* were collected on the campus of the State University of Campinas (Campinas, SP, Brazil). The testes were dissected and processed for light and transmission electron microscopy as described below.

Light microscopy

The specimens were fixed in aqueous Bouin solution for 12 h at 4°C, rinsed in distilled water, dehydrated in ethanol and

Correspondence to: Dr. Karina Mancini
Departamento de Biologia Celular, Instituto de Biologia, Universidade Estadual de Campinas (UNICAMP), CEP 13084-971, CP 6109, Campinas, SP, Brasil. Tel: (55) (19) 3788-6114, Fax: (55) (19) 3788-6111, E-mail: kazinhamancini@yahoo.com.br, heidi@unicamp.br

embedded in Technovit 7100 historesin. The tissues were sectioned at 1-2 μm, mounted on microscope slides and stained with toluidine blue, pH 4.0, or with Harris´s hematoxylin.

Transmission electron microscopy

Testes were fixed overnight in a solution containing 2.5% glutaraldehyde, 0.2% picric acid and 3% sucrose in 0.1 M sodium phosphate buffer, pH 7.2, at 4ºC. The tissues were post-fixed with 1% osmium tetroxide in the same buffer at 4ºC, dehydrated in acetone and embedded in epoxy resin. To obtain good preservation of the protein structures, the tissues were fixed for three days (according to Dallai and Afzelius [3]) in 2.5% glutaraldehyde and 1% tannic acid in 0.1 M phosphate buffer and contrasted for 3 h with 1% aqueous uranyl acetate at room temperature. The specimens were then dehydrated in acetone and embedded in epoxy resin. Ultrathin sections (20-60 nm) were stained with 2% uranyl acetate (20 min) and 2% lead citrate (7 min) prior to observation with a transmission electron microscope (Zeiss, Leo 906).

RESULTS

Light microscopy

The adult male reproductive tract of *E. hegesia* consisted of a single, fused, red, spherical testis, which contained cells in different developmental stages, with pre- and post-meiotic divisions. The testis was limited externally by tunica cells and was formed by follicles that enclosed several cysts in which apyrene and eupyrene spermatogenesis occurred (Fig. 1A). The two types of spermatozoa were never produced in the same cyst. Within these cysts, the germ cells that were surrounded by somatic (or cystic) cells (Fig. 1F,H) divided synchronously, which resulted in a uniform, side-by-side organization of spermatids, all at the same stage of differentiation.

Spermatogenesis advanced centripetally in the testis. The spermatogonia and spermatocyte cysts were located at the testis periphery (Fig. 1A). The spermatogonia, which possessed abundant dense cytoplasm and a spherical nucleus, formed dense, homogenous cysts (Fig. 1A,B). The spermatocytes were located around the cyst periphery and contained a large amount of cytoplasm, a spherical nucleus with scattered dense chromatin aggregates, and a prominent nucleolus (Fig. 1C).

The spermatids were uniformly distributed in large cysts and contained the nebenkern or mitochondrial complex [reviewed in 27 and 28] from which the mitochondrial derivatives were formed during tail elongation (Fig. 1D).

The first evidence to distinguish early apyrene from eupyrene spermatids was the presence of atypical nuclei in apyrene cells, which appeared as large, dense, amorphous, spherical structures (Fig. 1E). In contrast, eupyrene spermatids had a typical nucleus that elongated and became compacted during spermiogenesis (Fig. 1G,H).

In apyrene spermatozoa there was no nucleus at the anterior tip, since a degenerated nucleus, ready to be eliminated, was observed in the posterior tip of spermatid tails (Fig. 1F). The eupyrene spermatozoa had a very thin anterior region (Fig. 1H). Cysts containing both apyrene and eupyrene sperm were localized in the center of the testis and remained closely aligned (Fig. 1I).

Transmission electron microscopy

Apyrene spermiogenesis

Early apyrene spermatids were characterized by a spherical shape, a large cytoplasmic volume and, principally, by the presence of several micronuclei formed at the end of the second meiotic division (Fig. 2A). Initially, the micronuclei had an intact nuclear envelope with no pore complexes and surrounded clusters of dense chromatin (Fig. 2A). The micronuclei showed a heterogeneous chromatin distribution that varied in size and condensation, but became very dense during spermiogenesis. These micronuclei became dispersed in the cytoplasm, and gradually degenerated, causing disorganization of the chromatin and nuclear envelope and leaving an electron-lucid, degenerated ring (Fig. 2B,E). In elongated spermatids, the micronuclei were eliminated in vesicles at the posterior tip of the tail along with excess cytoplasm (Fig. 2F).

The cytoplasm of early apyrene spermatids contained several micronuclei and a basal body (or centriole) that had a dense covering at its anterior end and an axoneme extending from its distal end (Fig. 2G). In elongated spermatids, this basal body was initially topped by a short, thin layer (Fig. 2H) that developed into a dense cap over the anterior tip of the apyrene spermatozoa (Fig. 2I,J). This dense cap had two distinct regions: a dense internal material and an external ring that extended over the initial portion of the axoneme (Fig. 2J). This anterior portion of the elongated spermatids and spermatozoa was located in invaginations of the surface of the cystic cell (Fig. 2H,J).

The flagellum contained an axoneme and two mitochondrial derivatives. In apyrene sperm, the axoneme originated from the posterior tip of the basal body, beginning with the accessory microtubules (Fig.

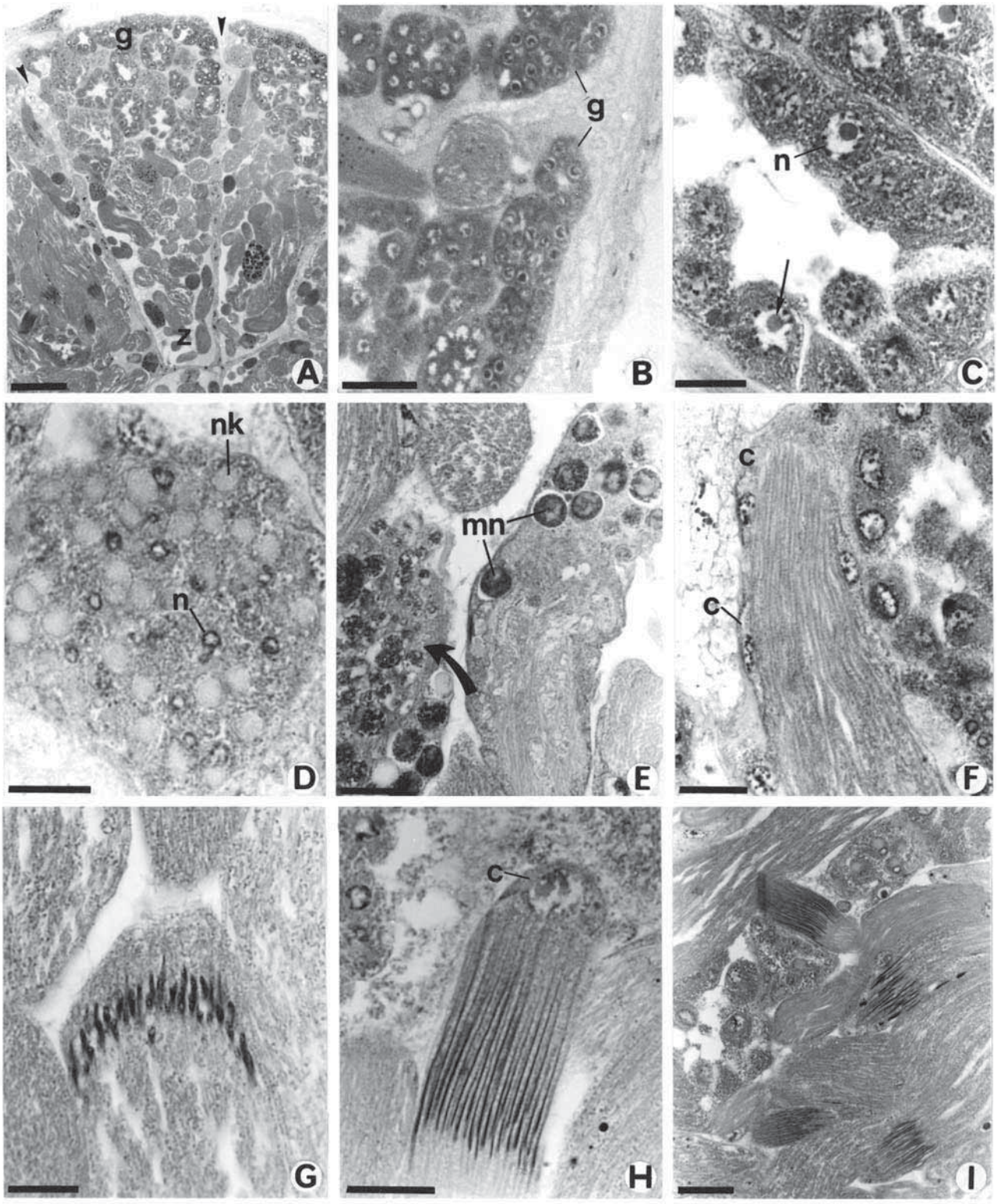

Figure 1. Light microscopy of *Euptoieta hegesia* testis. (**A**) Follicles limited by the tunica (**arrowhead**) with several cysts in different developmental stages. **g**-spermatogonia, **z**-spermatozoa. (**B**) Dense spermatogonial cysts (**g**) in the testis periphery. (**C**) Spermatocyte cysts with spherical nuclei (**n**) and evident nucleoli (**arrow**). (**D**) Spermatid cyst with spherical nuclei (**n**) and nebenkern (**nk**). (**E**) Elongated apyrene spermatid cyst with dense micronuclei (**mn**), degenerating cytoplasm and nuclei (**arrow**). (**F**) Apyrene spermatozoon cyst. Note the cystic cells (**c**) and the absence of a nucleus in the anterior region. (**G**) Elongated eupyrene spermatids with their nuclei in condensation and elongation processes. (**H**) Eupyrene spermatozoon cyst with very thin and compact nuclei. Cyst cell (**c**). (**I**) Eupyrene (with dense elongated nucleus) and apyrene (without nucleus) cysts in the center of the testis. Bars = 30 μm (A), 10 μm (B) and (I), 4 μm (C) to (H).

2K) and followed by the peripheral doublets (Fig. 2L) and by the central microtubules (Fig. 2M). The accessory microtubules and one of the central pair were generally electron-dense (Fig. 2K,M,O,P). In early spermatids, the axoneme initially consisted of a 9+2 microtubule organization, with nine peripheral doublets and two central microtubules (Fig. 2N), but eventually developed the nine accessory microtubules which branched off from the doublets, leading to the definitive 9+9+2 axoneme arrangement (Fig. 2N, inset).

The apyrene tail also contained two mitochondrial derivatives, which develop from the nebenkern. In spermatids with a 9+2 axoneme, the mitochondrial derivatives were located near the axoneme (Fig. 2N) and were initially very large.

In elongated spermatids, with a reduced cytoplasmic volume and 9+9+2 axoneme, the mitochondrial derivatives had a paracrystalline core and were surrounded by several microtubules (Fig. 2O). In the tail of late spermatids and spermatozoa, the mitochondrial derivatives were alike and had a well-defined, paracrystalline core which was made more distinct by the use of tannic acid (Fig. 2Q). Transversal sections of the initial portion of the axoneme showed the mitochondrial derivatives appearing one at a time, at different levels (Fig. 2J). The presence of supernumerary microtubules was frequent in late intratesticular apyrene spermatids (Fig. 2P).

In the posterior region of the spermatozoa, the mitochondrial derivatives terminated at different levels along the axoneme (1 and 2 in Fig. 2R). From this point onwards the axoneme became disorganized, first through the loss of the accessory microtubules (3 in Fig. 2R), followed by the central pair and finally the peripheral doublets (4 and 5 in Fig. 2R). The apyrene cyst (n = 20) contained an average of 256 (SD = 3) cells (Fig. 2S) and the spermatozoa was about 300 μm in length.

At the end of spermiogenesis, the apyrene spermatozoa were devoid of their nucleus and acrosome and contained a dense cap over the anterior tip. The flagellum possessed one axoneme with 9+9+2 microtubule arrangement and two mitochondrial derivatives that extended parallel to the axoneme.

Eupyrene spermiogenesis

Early eupyrene spermatids were characterized by abundant cytoplasm, a nebenkern next to the spherical nucleus, and an axoneme attached to the nucleus (Fig. 3A). In these cells, an acrosomal vesicle developed from the Golgi complex close to the spherical nucleus and attached to the nuclear envelope, opposite the axoneme (Fig. 3B,D). The vesicle initially contained a granular material (Fig. 3B) and then became a dense, compact, homogeneous structure (Fig. 3C) in contact with the plasma membrane next to a small extracellular appendage in the form of a dense cluster (Fig. 3D). In early elongating spermatids, the acrosome became elongated and migrated to a position in front of the axoneme (Fig. 3E); then later extended towards an attachment to a dense structure in the plasma membrane (Fig. 3F). The acrosome, which consisted of a dense external ring with an internal mass (Fig. 3F), eventually lost its attachment to the nuclear envelope and migrated to the anterior region of the elongated spermatid where it united with the plasma membrane (Fig. 3G). A single layer of microtubules surrounding this structure presumably contributed to the elongation process (Figs. 3H and 4A). The tubular acrosome complex eventually came to lie alongside the nucleus (Figs. 3J-M and 4A) and extended above it (Fig. 3H).

At the base of the head, the acrosome showed a dilated region with an internal mass (Fig. 3I). The attachment to the plasma membrane remained only during elongation (Fig. 3F-H,J). In elongated spermatids and spermatozoa, the acrosome extended

Figure 2. Transmission electron microscopy of apyrene cells. (**A**) Early apyrene spermatid with micronuclei (**mn**). (**B-E**) Micronuclei in various stages of degeneration. Note the electron-lucid degenerated ring (**arrow**). (**F**) Micronuclei (**mn**) elimination in the posterior tip of spermatids. (**G**) Longitudinal section of axoneme formation in an early spermatid. Note the anterior dense basal body (**b**). (**H**) Longitudinal section of a spermatid anterior tip with the early thin cap (**c**) above the axoneme (**ax**). (**I**) Longitudinal section of a spermatozoon anterior dense cap. (**J**) Transversal section of the anterior region of spermatozoa at different levels (**1-4**). Note that these anterior tips are embedded in the cystic cell (**c**). Mitochondrial derivatives appear at different levels (**arrow**). (**K-M**) Transversal section of the proximal region of the axoneme, showing the emergence of accessory microtubules, followed by the doublets and, finally, by the central pair, respectively (**arrow**). (**N**) Spermatid tail with a large cytoplasmic volume. Note the 9+2 axoneme (**ax**) with projections (**arrow**) and two mitochondrial derivatives (**md**). An early 9+9+2 axoneme is also shown (**inset**). (**O**) Late spermatid tail with 9+9+2 axoneme and mitochondrial derivatives containing small paracrystalline cores (**arrows**). Note also the microtubules (**arrowhead**). (**P,Q**) Spermatozoon tails fixed by conventional and tannic acid methods (P and Q, respectively). Note the differing densities in the axonemal microtubules (**arrowheads**). Mitochondrial derivatives (**md**) with paracrystalline core (**arrow**). Note the supernumerary microtubule in P (**small arrow**). (**R**) Transversal sections of sperm tails sectioned at progressively posterior levels (**1-5**). (**S**) Apyrene cyst. Bars = 1 μm (A) to (F) and (S), 0.3 μm (G) to (R).

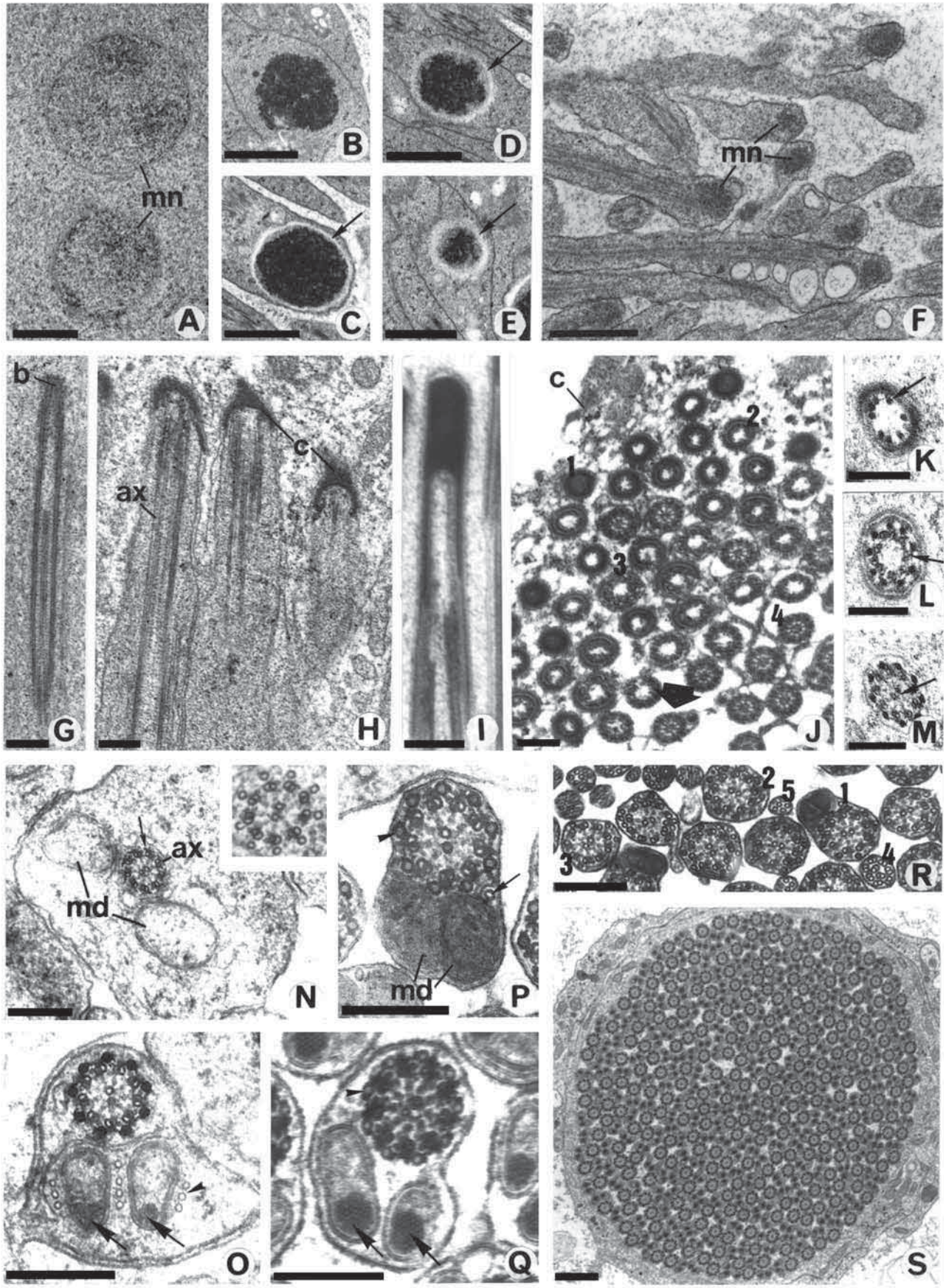
A
mn
B
C
D
E
F
mn
G
b
H
ax
c
I
J
c
1
2
3
4
K
L
M
N
ax
md
P
md
O
Q
R
2
5
1
3
4
S

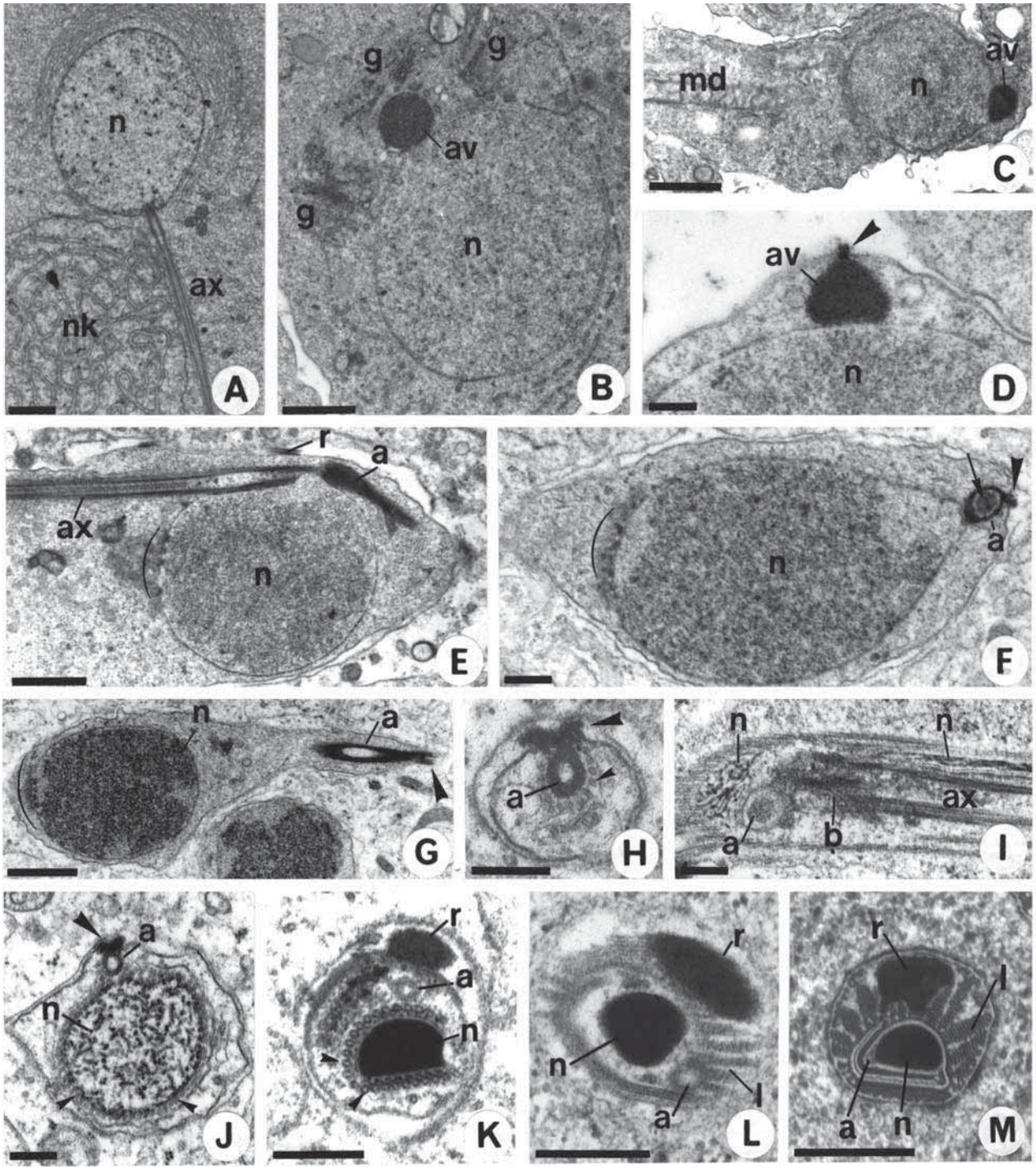

Figure 3. Transmission electron microscopy of eupyrene cells. (**A**) Early spermatid with spherical nucleus (**n**), axoneme (**ax**) attached posteriorly to the nucleus and nebenkern (**nk**). (**B,C**) Spermatids with spherical nucleus (**n**) and acrosomal vesicle (**av**) attached anteriorly. **g**-Golgi complex, **md**-mitochondrial derivatives. (**D**) Acrosomal vesicle (**av**) attached to the nucleus (**n**) and to the plasma membrane (**arrowhead**). (**E**) Elongated spermatid with axoneme (**ax**) and elongated acrosome (**a**) attached to the nucleus (**n**). The nuclear pore complex area (**arc**) and the reticular appendage (**r**) are also seen. (**F**) Elongated spermatid with tubular acrosome (**a**), attached to the nucleus (**n**) and plasma membrane (**arrowhead**). Note also the nuclear pore complex area (**arc**), the compacted chromatin and the acrosomal mass (**arrow**). (**G**) Elongating spermatid in which the tubular acrosome (**a**) is not attached to the nucleus (**n**) but still remains attached to the plasma membrane (**arrowhead**). Note the nuclear pore complex area (**arc**) and the rather dense chromatin. (**H**) Anterior tips of spermatid with the tubular acrosome (**a**) surrounded by microtubules (**small arrowhead**) and attached to the plasma membrane (**large arrowhead**). (**I**) Longitudinal section of the nuclear base showing the dilated acrosomal region (**a**) and the nucleus (**n**), that extends alongside the axoneme (**ax**) and basal body (**b**). (**J-M**) Transverse sections of different developmental stages (spermatids to spermatozoa) showing the chromatin condensation and appendage modifications. a-acrosome, **arrowhead**-microtubules, **n**-nucleus, **r**-reticular, **l**-lacinate appendages. Bars = 1.5 μm (A), 1 μm (B), (C), (E) and (G), 0.3 μm (D), (F) and (H) to (M).

parallel to the nucleus, with no membrane attachment (Fig. 3K-M).

Simultaneously with acrosome formation, the nucleus underwent changes in its shape, chromatin organization and nuclear pores. In early spermatids with an acrosomal vesicle, the nucleus was large and spherical with dispersed chromatin (Fig. 3B-D). Later, the nucleus elongated, the chromatin condensed and the pore complexes became concentrated in the area adjacent to the axoneme (Fig. 3E-G). These pore complexes were later eliminated from the spermatozoon. The chromatin showed large, dense aggregates (Fig. 3F,G) that were arranged into fibers (Fig. 3I,J) to become a homogeneous, compact material in very elongated spermatids and spermatozoa (Fig. 3K-M). The compact nucleus extended parallel to the tubular acrosome (Fig. 4A) and laterally to the initial portion of the axoneme (Figs. 3I and 4B,C). In this process, there was also a single layer of microtubules surrounding the nucleus (Figs. 3J,K and 4A). In addition to the acrosome and nucleus, two types of extracellular appendages, reticular and lacinate appendages, were observed (Fig. 3M). Both extended to the tail and were well-developed in the anterior region (Figs. 3M and 4C).

The reticular appendage was a single dense rod that was formed in early spermatids. This structure served as a marker to distinguish early apyrene and eupyrene spermatid tails. In the tail, this appendage initially appeared as a slender rod with an intra and extracellular portion (Fig. 4D). During early acrosome formation, in the anterior region of the sperm, there was an apparent association between these two structures in the plasma membrane (Fig. 3D-H,J). In late spermatids and spermatozoa, the reticular appendage was large in the head (Figs. 3K-M and 4A,C,G) and condensed in the tail (Fig. 4E-F,H-I), and was anchored to the plasma membrane by bridges (Fig. 4E,H).

The lacinate appendages were striated structures that surrounded the cell membrane. These structures were formed in late spermatids, after the reticular appendage had formed (Figs. 3L and 4F). In the anterior region of the sperm, the lacinate appendages covered almost all of the plasma membrane (Figs. 3M and 4C,G) while in the posterior region they were attached near the mitochondrial derivatives.

The tail contained an axoneme, two mitochondrial derivatives and the extracellular appendages. The mitochondrial derivatives were formed from the nebenkern (Fig. 3A), as in the apyrene cell. The axoneme arose from the basal body which, in early spermatids, was anchored to the nucleus on the side opposite to the acrosome (Fig. 3A). This basal body contained a dense mass that surrounded the microtubules (Fig. 4B). In spermatids, the tail had abundant cytoplasm, a 9+2 axoneme and two mitochondrial derivatives. With the assembly of the accessory microtubules, the axoneme acquired a 9+9+2 organization similar to that of apyrene cells (Fig. 4C-I). The mitochondrial derivatives were large and still surrounded by microtubules at this stage (Fig. 4D,E).

In late spermatids and spermatozoa, the cytoplasm was reduced and the reticular appendage was completely extracellular and anchored to the membrane (Fig. 4E,H), and had a paracrystalline organization (Fig. 4F,H). In the complete axoneme, the accessory and central microtubules were electron-dense (Fig. 4D,I). However, with tannic acid fixation, the accessory microtubules became translucent (Fig. 4E-F,H). The mitochondrial derivatives were closely packed and cytoplasmic microtubules were rare or absent (Fig. 4H,I). The eupyrene cyst (n = 20) contained an average of 256 ± 3 (mean ± SD) cells (Fig. 4J) and the spermatozoa measured about 600 μm in length.

At the end of spermiogenesis, the eupyrene spermatozoa contained a nucleus and a tubular acrosome in the head region and the flagellum consisted of an axoneme with a 9+9+2 microtubule arrangement and two mitochondrial derivatives that extended parallel to the axoneme. These spermatozoa also possessed lacinate and reticular extracellular appendages, exclusive to this order, which extended along the entire length of the sperm.

DISCUSSION

Spermiogenesis in *E. hegesia* was similar to that of other lepidopteran species [2,11,13,16,19-21,24,39,40]. In this insect order, sperm morphology is highly conserved between species and spermiogenesis follows a similar pattern.

Light microscopy

Numerous studies have described lepidopteran spermatogenesis and spermiogenesis based on light microscopy of thin sections or sperm suspensions [2,11,13,16,20,31]. However, all of these studies used larval stages and some also used pupae, mainly

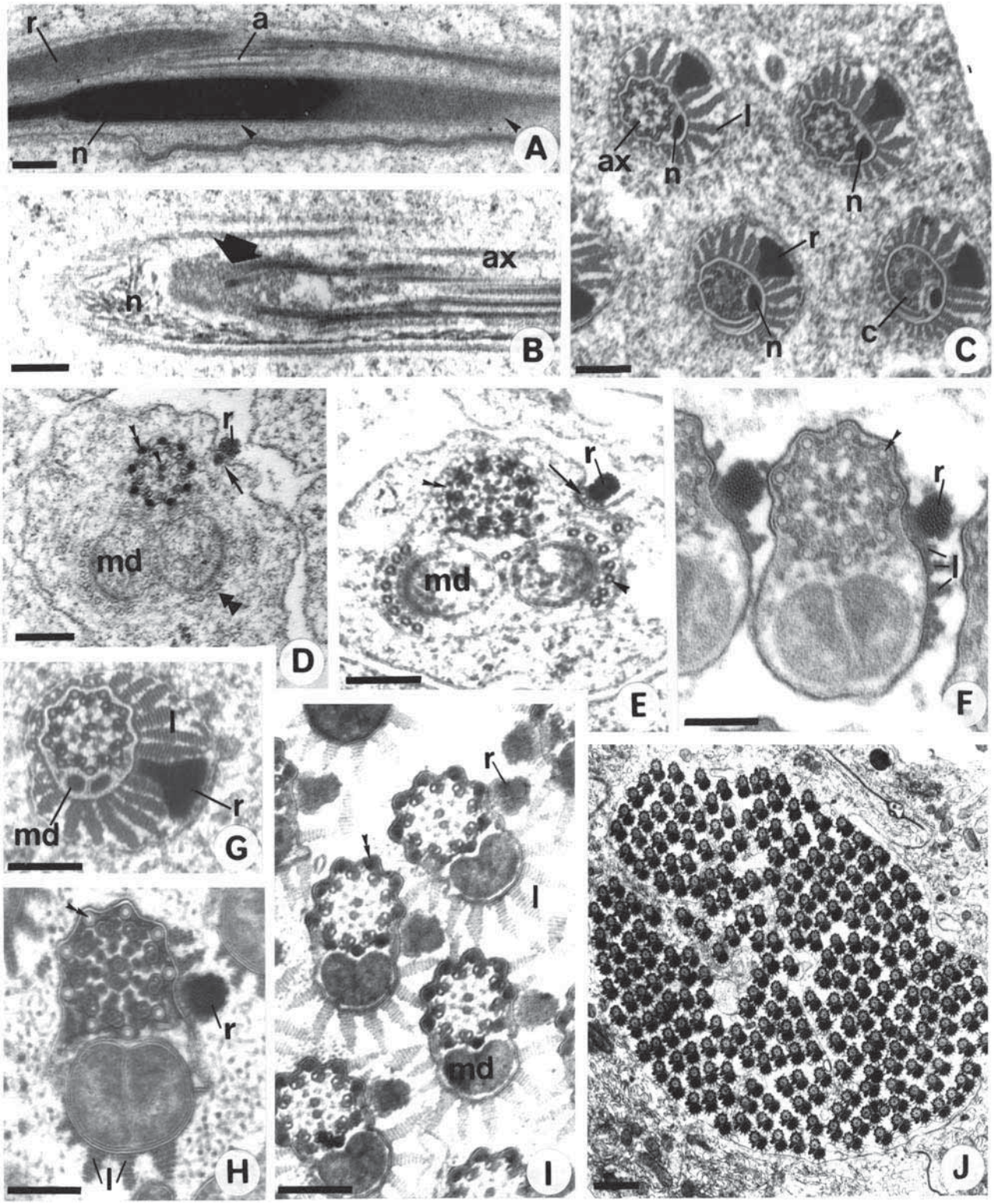

Figure 4. Transmission electron microscopy of eupyrene cells. (**A**) Longitudinal section of the anterior region showing the dense nucleus (**n**) with several microtubules (**arrowheads**), tubular acrosome (**a**) and reticular appendage (**r**). (**B**) Longitudinal section of the nucleus-tail transition region, showing the amorphous mass in and around the basal body (**arrow**) but anterior to the axoneme (**ax**), and the nucleus (**n**) lying alongside the axoneme. (**C**) Transverse section of the nucleus-tail transition region showing the nucleus (**n**), the centriole (**c**) and axoneme (**ax**). Note the well-developed lacinate (**l**) and reticular (**r**) appendages. (**D**) Tail of a spermatid with a 9+9+2 axoneme and two mitochondrial derivatives. The reticular appendage (**r**) possesses internal (**arrow**) and external regions. Note the microtubules (**large double arrowhead**) around the mitochondrial derivatives and the dense accessory (**small double arrowhead**) and central microtubules (**arrowhead**). (**E**) Tail of a spermatid with a 9+9+2 axoneme and mitochondrial

derivatives fixed with tannic acid. Note the microtubules (**arrowhead**) around the mitochondrial derivatives (**md**) and the electron-lucid accessory microtubules (**double arrowhead**). A reticular appendage (**r**) with an external region anchored to the plasma membrane (**arrow**) can also be seen. (**F**) Late spermatid fixed with tannic acid. Note the early lacinate appendage formation (**l**), the paracrystalline arrangement of the reticular appendage (**r**) and the electron lucid accessory microtubules (**double arrowhead**). (**G**) Transverse section of the anterior region of spermatozoon axoneme showing the well-developed lacinate (**l**) and reticular (**r**) appendages, a 9+9+2 axoneme and mitochondrial derivative tips (**md**). (**H,I**) Spermatozoon tail fixed with tannic acid and conventional methods, respectively. Note the difference in electron density between the axoneme microtubules (**double arrowhead**), and the morphology of the lacinate (**l**) and reticular (**r**) appendages. **md**-mitochondrial derivatives. (**J**) Eupyrene cyst. Bars = 0.2 μm (A) to (I), 1.25 μm (J).

because the initial developmental stages contain all germ cell types. In the present study only adult males were examined and all stages of spermatogenesis were found (Fig. 1A-I). *Euptoieta hegesia* belongs to the subfamily Heliconiinae, whose members have a long adult lifespan in which spermatogenesis continues in the imago, as observed in *Methona themisto* [2] and *Calpodes ethlius* [20].

The general organization of the testis described here, with several follicles containing apyrene and eupyrene cysts and an apical-basal direction of spermatogenesis, was similar to that reported for other species. Apyrene and eupyrene cells were distinguished by the presence of micronuclei in apyrene spermatids. In *C. ethlius*, significant differences in the size of apyrene and eupyrene cysts allowed them to be distinguished when they were still secondary spermatocytes [20].

Transmission electron microscopy

Apyrene spermiogenesis

Loss of the nucleus, modification in the nebenkern, anterior dense cap formation and elongation of the tail are processes associated with apyrene spermiogenesis. In *Alabama argillacea*, apyrene spermiogenesis has been divided into six stages [24], but we observed continuous maturation, without the sub-divisions reported in other studies.

The micronuclear morphology varies among species. In *E. hegesia,* these structures are heterogeneous in size and have dense amorphous chromatin. In *Ephestia cautella* [9], the micronuclei are of two morphologically distinct types, as also occurs in *A. argillacea* [24]. The differences observed in *E. hegesia* were related to the process of degeneration and not the occurrence of distinct types. The presence of membranes covering the micronuclei, as reported for *A. argillacea* [24], *E. cautella* [9] and *C. ethlius* [21], was not observed here.

The elimination of micronuclei from the posterior tail region in *E. hegesia* was similar to that reported for *E. cautella* [9], *C. ethlius* [21] and *A. argillacea* [24]. In *Bombyx mori* [18], peristaltic contractions of the sperm cysts was detected in late spermatogenesis. These contractions result in the elimination of the cytoplasm of eupyrene sperm and of the cytoplasm and nuclei of the apyrene sperm from the posterior end of the sperm.

The anterior dense cap of *E. hegesia* was similar to that observed in most lepidopteran species, including *Trichoplusia ni* [30], *B. mori* [8], *C. ethlius* [21], *A. argillacea* [25], *Atrophaneura alcinous* [19] and many other species described by Jamieson [14,15] and Phillips [26]. Although this structure is well-known, the formation of the dense cap in apyrene spermatids, as seen in *E. hegesia*, has been observed only in *B. mori* [10] and *A. argillacea* [24].

The presence of a basal body below the dense cap and above the axoneme appears to be a characteristic feature of the Lepidoptera [8,10,14,15,21,24,40].

The mitochondrial derivatives of *E. hegesia* apyrene sperm were smaller, than those of eupyrene sperm, and had a paracrystalline core, as also observed in *B. mori* [8], *A.argillacea* [25] and other species studied by Phillips [26].

Eupyrene spermiogenesis

Acrosomal development, nuclear changes, modifications in the nebenkern, extracellular appendage formation and elongation of the tail were events associated with eupyrene spermiogenesis.

The tubular acrosome of *E. hegesia* was similar to that of most lepidopteran species [19,21,24]. The formation of this acrosome and its migration to the membrane were described in *C. ethlius* [21], in a process similar to that found in *E. hegesia*. The association between the acrosome and the plasma membrane in a small dense extracellular cluster, probably representing the early reticular appendage, has also been observed in *A. argillacea* [24], *B. mori* [41,42] and *C. ethlius* [21].

As to the nuclear changes in *E. hegesia*, the chromatin was evenly distributed as dense areas in early spermatids, followed by arrangement into a fibrous network in elongating spermatids and, finally,

as a very dense, homogenous material in the spermatozoa. In *A. argillacea* [24], *C. ethlius* [21] and *B. mori* [10,17,38] the process of chromatin condensation begins at the nuclear periphery, in contrast to that observed here.

The alterations in the spermatid head of *E. hegesia,* including the locations of the acrosome, nucleus and basal body were similar to these reported by Friedländer and Wahrman [10], Lai-Fook [21], Medeiros [24] and Zylberberg [43].

The lacinate and reticulate appendages are exclusive structures of the order Lepidoptera and are present in all species examined so far, except in the Micropterygidae [12,35]. These extracellular appendages are morphologically very similar among species.

The reticular appendage is the principal characteristic for differentiating between apyrene and eupyrene spermatid tails in the early stages of development. The morphological, dimensional and organizational modifications seen in this appendage during spermiogenesis in *E. hegesia* agreed with the observations for *C. ethlius* [21] and *A. argillacea* [23,24]. The reticular paracrystalline structure, revealed by tannic acid, has also been reported in *A. argillacea* [24] and *Apopestes spectrum* [15]. The use of tannic acid and other cytochemical observations suggest that the reticular appendage is composed of glycoproteins (data not shown). We believe this structure is involved in the packaging of eupyrene sperm by helping to maintain the close association of spermatozoa.

The lacinate appendages assembled on the late spermatids also showed a regular structure with tannic acid. The number and shape of these structures vary among the species studied. A study of the effects of vinblastine on the lacinate appendages of *Ephestia cautella* demonstrated that these structures became poorly resolved and disappeared in the presence of this substrate, which suggested that tubulin may be a component of these appendages [7]. In agreement with this, the use of tannic acid (indicated for microtubule preservation) in *E. hegesia* and *A. spectrum* [15], resulted in the observation of a regular structure. However, although these appendages contain protein, we do not believe they are composed of tubulin. We agree with Medeiros [23,24], that these appendages are involved in the organization of sperm sheaths, and that they help to maintain a close association between sperm cells.

Both of the mitochondrial derivatives in the axoneme were of equal diameter, as also seen in *A. alcinous* [19]. However, many species have unequal mitochondrial derivatives [15]. No paracrystalline core was observed in eupyrene mitochondrial derivatives. The eupyrene cysts of *E. hegesia* had 256 sperm cells, as do those of *C. ethlius* [21], *A. argillacea* [23,24], *A. alcinous* [19] and all species studied by Phillips [26].

In conclusion, dichotomic spermiogenesis in the order Lepidoptera is very complex and involves events such as the loss of the nucleus and cap formation in apyrene spermiogenesis, and the development of elaborate extracellular appendages in eupyrene spermiogenesis. This study of dichotomic spermiogenesis in *E. hegesia* corroborates and complements reports in the literature since it has shown intermediate stages in the formation of some structures, such as the acrosome, axoneme and extracellular appendages.

ACKNOWLEDGMENTS

The authors thank A.V.L. Freitas for supplying the butterflies. This research was supported by the Brazilian agency FAPESP (grants 98/03200-9 and 01/01049-6).

REFERENCES

1. Cook PA, Wedell N (1999) Non-fertile sperm delay female remating. *Nature* **397**, 486.
2. Corsatto-Alvarenga LBF, Cestari NA, Ribeiro AF (1987) Apyrene and eupyrene spermatogenesis in *Methona themisto* (Lepidoptera: Ithominae). *Rev. Bras. Genét.* **10**, 655-672.
3. Dallai R, Afzelius BA (1990) Microtubular diversity in insect spermatozoa: results obtained with a new fixative. *J. Struct. Biol.* **103**, 164-179.
4. Drummond BA (1984) Multiple mating and sperm competition in the Lepidoptera. In: *Sperm Competition and the Evolution of Animal Mating Systems* (Smith RL, ed). pp. 291-370. Academic Press: London.
5. Fain-Maurel MA (1966) Acquisition récentes sur les spermatogenèses atypiques. *Ann. Biol.* **5**, 513-564.
6. Friedländer M, Benz G (1981) The apyrene-eupyrene dichotomous spermatogenesis of Lepidoptera. Organ culture study on the timing of apyrene commitment in the codling moth. *Int. J. Invert. Reprod.* **3**, 113-120.
7. Friedländer M, Gershon J (1978) Reaction of surface lamella of moth spermatozoa to vinblastine. *J. Cell Sci.* **30**, 353-361.
8. Friedländer M, Gitay H (1972) The fate of the normal anucleated spermatozoa in inseminated females of the silkworm *Bombyx mori*. *J. Morphol.* **138**, 121-129.
9. Friedländer M, Miesel S (1977) Spermatid enucleation during the normal atypical spermiogenesis of the warehouse moth *Ephestia cautella*. *J. Submicrosc. Cytol.* **9**, 173-185.
10. Friedländer M, Wahrman J (1971) The number of centrioles in insect sperm: a study in two kinds of differentiating silkworm spermatids. *J. Morphol.* **134**, 383-397.

11. Garbini CP, Imberski RB (1977) Spermatogenesis in *Ephestia kuehniella* (Lepidoptera, Pyralididae). *Trans. Am. Micros. Soc.* **96**, 189-203.
12. Hamon C, Chauvin G (1992) Ultrastructural analysis of spermatozoa of *Korscheltellus lupulinus* L. (Lepidoptera: Hepialidae) and *Micropterix calthella* L. (Lepidoptera: Micropterigidae). *J. Insect Morphol. Embryol.* **21**, 149-160.
13. Holt GG, North DT (1970) Spermatogenesis in the cabbage looper *Trichoplusia ni* (Lepidoptera: Noctuidae). *Ann. Entomol. Soc. Am.* **63**, 501-507.
14. Jamieson BGM (1987) *The Ultrastructure and Phylogeny of Insect Spermatozoa*. Cambridge University Press: Cambridge.
15. Jamieson BGM, Dallai R, Afzelius BA (1999) *Insects: their Spermatozoa and Phylogeny.* Science Publishers: Enfield, New Hampshire.
16. Katsuno S (1989) Spermatogenesis and the abnormal germ cells in Bombycidae and Saturniidae. *J. Fac. Agr. Hokkaido Univ.* **64**, 21-34.
17. Kawamura N, Yamashiki N, Bando H (1998) Behavior of mitochondria during eupyrene and apyrene spermatogenesis in the silkworm, *Bombyx mori* (Lepidoptera) investigated by fluorescence *in situ* hybridization and electron microscopy. *Protoplasma* **202**, 223-231.
18. Kawamura N, Yamashiki N, Saitoh H, Sahara K (2000) Peristaltic squeezing of sperm bundles at the late stage of spermatogenesis in the silkworm, *Bombyx mori*. *J. Morphol.* **246**, 53-58.
19. Kubo-Irie M, Irie M, Nakazawa T, Mohri H (1998) Morphological changes in apyrene and eupyrene spermatozoa in the reproductive tract of the male butterfly *Atrophaneura alcinous* Klug. *Invert. Reprod. Dev.* **34**, 259-269.
20. Lai-Fook J (1982a) Testicular development and spermatogenesis in *Calpodes ethlius* Stoll (Hesperidae: Lepidoptera). *Can. J. Zool.* **60**, 1161-1171.
21. Lai-Fook J (1982b) Structural comparison between eupyrene and apyrene spermiogenesis in *Calpodes ethlius* (Hesperiidae: Lepidoptera). *Can. J. Zool.* **60**, 1216-1230.
22. Leviatan R, Friedländer M (1979) The eupyrene-apyrene dichotomous spermatogenesis of Lepidoptera. The relationship with postembryonic development and the role of the decline in juvenile hormone titer toward pupation. *Dev. Biol.* **68**, 515-524.
23. Medeiros M (1986) *Caracterização ultra-estrutural de espermatozóides eupirenes e apirenes de Alabama argillacea Hübner, 1818 (Lepidoptera: Noctuidae), ao nível dos testículos e das vias genitais de imagos machos e fêmeas até a espermateca.* (Masters dissertation). Instituto de Biologia, Universidade Estadual de Campinas. 122p.
24. Medeiros M (1997) *Estudo ultra-estrutural da espermiogênese dicotômica de Alabama argillacea Hübner, 1818.* (Doctoral thesis). Instituto de Biociências, Universidade Estadual de São Paulo. 142p.
25. Medeiros M, Silveira M (1996) Ultrastructural study of apyrene spermatozoa of *Alabama argillacea* (Insecta, Lepidoptera, Noctuidae) with tannic acid containing fixative. *J. Submicrosc. Cytol. Pathol.* **28**, 133-140.
26. Phillips DM (1971) Morphogenesis of the lacinate appendages of lepidopteran spermatozoa. *J. Ultrastruct. Res.* **34**, 567-585.
27. Pratt SA (1968) An electron microscope study of nebenkern formation and differentiation in spermatids of *Murgantia histrionica* (Hemiptera, Pentatomidae). *J. Morphol.* **126**, 31-66.
28. Pratt AS (1970) Formation and differentiation of the nebenkern in spermatids of a hemipteran insect, *Murgantia histrionica*. In: *Comparative Spermatology* (Baccetti B, ed). pp. 301-311. Academic Press: New York.
29. Osanai M, Kasuga H, Aigaki T (1987) Physiological role of apyrene spermatozoa of *Bombyx mori*. *Experientia* **43**, 593-596.
30. Riemann JG (1970) Metamorphosis of the cabbage looper *Trichoplusia ni* during passage from the testes to the female spermatheca. In: *Comparative Spermatology* (Baccetti B, ed). pp. 321-331. Academic Press: New York.
31. Scheepens MHM, Wysoki M (1985) Testicular development, spermatogenesis and chromosomes of *Boarmia selenaria* sciff (Lepidoptera: Geometridae). *Int. J. Invert. Reprod. Dev.* **8**, 337-348.
32. Silberglied RE, Shepherd JG, Dickinson JL (1984) Eunuchs: the role of apyrene sperm in lepidoptera? *Am. Nat.* **123**, 255-265.
33. Snook RR (1997) Is the production of multiple sperm types adaptive? *Evolution* **51**, 797-808.
34. Snook RR (1998) The risk of sperm competition and the evolution of sperm heteromorphism. *Anim. Behav.* **56**, 1497-1507.
35. Sonnenschein M, Hauser CL (1990) Presence of only eupyrene spermatozoa in adult males of the genus *Micropteryx* Hubner and its phylogenetic significance. *Int. J. Insect Morphol. Embryol.* **19**, 269-276.
36. Wedell N, Cook PA (1999a) Butterflies tailor their ejaculate in response to sperm competition risk and intensity. *Proc. R. Soc. Lond. B Biol. Sci.* **266**, 1033-1039.
37. Wedell N, Cook PA (1999b) Strategic sperm allocation in the small white butterfly *Pieris rapae* (Lepidoptera: Pieridae). *Funct. Ecol.* **13**, 85-93.
38. Wolf KW (1992) Spindle membranes and microtubules are coordinately reduced in apyrene relative to eupyrene spermatocytes of *Inachis io* (Lepidoptera: Nymphalidae). *J. Submicrosc. Cytol. Pathol.* **24**, 381-394.
39. Wolf KW, Baumgart K, Traut W (1987) Cytology of Lepidoptera. II. Fine structure of eupyrene primary spermatocytes in *Orgyia thyellina*. *Eur. J. Cell Biol.* **44**, 57-67.
40. Yamashiki N, Kawamura N (1997) Behaviors of nucleus, basal bodies and microtubules during eupyrene and apyrene spermiogenesis in the silkworm *Bombyx mori* (Lepidoptera). *Dev. Growth Differ.* **39**, 715-722.
41. Yasuzumi G, Oura C (1964) Spermatogenesis in animals as revealed by electron microscopy. XIII. Formation of a tubular structure and two bands in the developing spermatid of the silkworm *Bombyx mori* Linné. *Z. Zellforsch. Mikrosk. Anat.* **64**, 210-226.
42. Yasuzumi G, Oura C (1965) Spermatogenesis in animals as revealed by electron microscopy. XIV. The fine structure of the clear band and tubular structure in late stages of development of spermatids of the silkworm *Bombyx mori* Linné. *Z. Zellforsch. Mikrosk. Anat.* **66**, 182-196.
43. Zylberberg L (1969) Contribution a l'étude de la double spermatogenèse chez un lépidoptère (*Pieris brassicae* L., Pieridae). *Ann. Sci. Nat. Zool.* **11**, 569-626.

Received: October 1, 2003
Accepted: November 6, 2003